Heterologous Production, Isolation, Characterization and Crystallization of a Soluble Fragment of the NADH:Ubiquinone Oxidoreductase (Complex I) from *Aquifex aeolicus*[†]

Markus Kohlstädt,[‡] Katerina Dörner,[‡] Ramona Labatzke,[‡] Cengiz Koç,[‡] Ruth Hielscher,[§] Emile Schiltz,[‡] Oliver Einsle,[‡] Petra Hellwig,[§] and Thorsten Friedrich*[,‡]

Institut für Organische Chemie and Biochemie, Albert-Ludwigs-Universität, Albertstrasse 21, 79104 Freiburg, Germany, and Institut de Chimie UMR 7177, Laboratoire de spectroscopie vib. et electrochimie des biomolecules, CNRS, Université Louis Pasteur, 4, rue Blaise Pascal, 67070 Strasbourg, France

Received July 11, 2008

ABSTRACT: The proton-pumping NADH:ubiquinone oxidoreductase (complex I) is the first enzyme complex of the respiratory chains in many bacteria and most eukaryotes. It is the least understood of all, due to its enormous size and unique energy conversion mechanism. The bacterial complex is in general made up of 14 different subunits named NuoA−N. Subunits NuoE, -F, and -G comprise the electron input part of the complex. We have cloned these genes from the hyperthermophilic bacterium *Aquifex aeolicus* and expressed them heterologously in *Escherichia coli*. A soluble subcomplex made up of NuoE and NuoF and containing the NADH binding site, the primary electron acceptor flavin mononucleotide (FMN), the binuclear iron−sulfur cluster N1a, and the tetranuclear iron−sulfur cluster N3 was isolated by chromatographic methods. The proteins were identified by N-terminal sequencing and mass spectrometry; the cofactors were characterized by UV/vis and EPR spectroscopy. Subunit NuoG was not produced in this strain. The preparation was thermostable and exhibited maximum NADH/ferricyanide oxidoreductase activity at 85 °C. Analytical size-exclusion chromatography and dynamic light scattering revealed the homogeneity of the preparation. First attempts to crystallize the preparation led to crystals diffracting more than 2 Å.

The proton-pumping NADH:ubiquinone oxidoreductase, also called respiratory complex I,[1] is the first enzyme of the electron transfer chains in the mitochondria of most eukaryotes and the cytoplasmic membranes of many bacteria. It catalyzes the transfer of two electrons from NADH to ubiquinone via one flavin mononucleotide (FMN) and a series of iron−sulfur (Fe−S) clusters. The electron transfer is coupled to the translocation of four protons across the membrane, thereby contributing to the membrane potential (*1*−*3*). In eukaryotes, complex I consists of 45 different subunits resulting in a molecular mass of about 1 MDa (*4*). The bacterial homologue contains the same cofactors and catalyzes the same reaction as the mitochondrial complex, but it comprises only 14 subunits. Because of that, the bacterial complex I is regarded as a simple model for the eukaryotic enzyme (*5*). Electron microscopy revealed that complex I is made up of a peripheral and a membrane arm (*6*−*8*). The FMN and the Fe−S clusters are located in the peripheral arm of the complex (*5, 9, 10*). The structure of this arm from the *Thermus thermophilus* complex I was recently determined (*10*). From secondary structure prediction and electron microscopy, it is expected that the membrane arm contains 61 transmembrane α-helices (*8, 11*). The arm most likely participates in quinone binding and is involved in proton translocation (*12*−*15*).

The hyperthermophilic, microaerophilic, and obligate chemolithoautotrophic eubacterium *Aquifex aeolicus* grows at temperatures up to 95 °C and is one of the first organisms to branch out in the domain of the eubacteria (*16*−*18*). The genome of the hyperthermophilic bacterium was the first to have been sequenced, revealing the presence of 24 *nuo* genes coding for subunits of complex I. Seven genes are present in duplicate form and two as triplicates (*19*). As in *Escherichia coli* and a few other bacteria, the genes *nuoC* and *nuoD* are fused to one gene, *nuoD2* (*19, 20*). Thirteen of the 24 genes most likely code for complex I, while the function of the remaining duplicate and triplicate *nuo* genes is not known. It is not even known whether the genes are expressed. However, the presence of a thermostable energy-converting NADH:ubiquinone oxidoreductase in the cytoplasmic membranes of *A. aeolicus* has been demonstrated (*21*). Unlike most other bacteria, the 13 *nuo* genes are not organized within one operon or gene cluster but are present in three loci: *nuoE* and *F*, *nuoG*, and *nuoA2*, *B*, *D2*, *H1*, *I1, J1*, *K1*, *L1*, *M1*, and *N1*. Complex I was isolated from *A. aeolicus*, confirming the presence of a 13 subunit complex (*22*). The subunits NuoD2, E, F, G, H1, I1, and M1 were identified in

[†] This work is supported by the Volkswagen Stiftung.

* Corresponding author. Tel: +49-(0)761-203-6060. Fax: +49-(0)761-203-6096. E-mail: thorsten.friedrich@uni-freiburg.de.

[‡] Albert-Ludwigs-Universität.

[§] Université Louis Pasteur.

[1] Abbreviations: complex I, proton-pumping NADH:ubiquinone oxidoreductase; DSL, dynamic light scattering; EPR, electron paramagnetic resonance; FMN, flavin mononucleotide; Fe−S, iron−sulfur; MES, 2-(*N*-morpholino)-ethanesulfonic acid; MOPS, 3-(*N*-morpholino)-propanesulfonic acid; vis, visible; SDS−PAGE, sodium dodecylsulfate polyacrylamide gel electrophoresis.

10.1021/bi801307n CCC: $40.75
Published on Web 11/12/2008

the preparation by means of mass spectrometry and N-terminal sequencing. It was shown that the electron input part of this preparation, the so-called NADH dehydrogenase fragment consisting of subunits NuoE, F, and G (*23, 24*), is stable up to 80 °C in the presence of SDS (*22*). This extraordinary stability makes the fragment an ideal candidate for X-ray structure analysis. However, the growth yield of *A. aeolicus* (*16*) and the yield of the complex I preparation (*22*) are both very low.

To overcome these problems, we have overexpressed the *A. aeolicus* genes *nuoE*, *F*, and *G* heterologously in *E. coli*. The subunits NuoE and F were produced and assembled with the cofactors as one subcomplex in the cytoplasm, but not NuoG. The NuoEF subcomplex was purified to homogeneity, characterized, and crystallized.

MATERIALS AND METHODS

Materials and Strains. For gene expression, *E. coli* strain Rosetta(DE3)pLacI and the plasmid pETBlue-1 (both Merck Biosciences, Nottingham) were used. *E. coli* strain DH5α (*25*) was used for the preparation of DNA. During the growth of the Rosetta strain, chloramphenicol was added to the medium at 34 μg/mL. For maintenance of the expression plasmid, ampicillin was added to 100 μg/mL.

Construction of Expression Vectors. A. aeolicus cells were kindly provided by R. Huber, University of Regensburg. For extraction and manipulation of DNA, standard methods according to procedures in ref *26* were used. Primer Pa (5′-TAT GTT TAA AAC GGA GTT TGA ATT TCC CG-3′) and primer Pb (5′-*TTT TTC GAA CTG CGG GTG GCT CCA GCT AGC* AAG GGG AA GGG AAG CAG ATT TCT TTC-3′) were used to amplify *nuoEF* from genomic *A. aeolicus* DNA. Primer Pb contains the inverted sequence of the *Strep* tag II including two spacer amino acids, shown in italics. Primers Pc (5′-*GCT AGC TGG AGC CAC CCG CAG TTC GAA AAA* TAA AAT CGA ATT CAA GGA GGT TGA TAT GTC C-3′) and Pd (5′-AGT TCG CTC AGC CTA AAC ACT CCT TTC GTA GTA AAC C-3′) were used to amplify *nuoG* from genomic *A. aeolicus* DNA. Primer Pc contains the sequence of the *Strep* tag II including two spacer amino acids, shown in italics. Primer Pd was designed to introduce a *Bpu*1102I restriction site behind the stop codon of *nuoG* (underlined). Both amplicons were used in an overlap extension (OE) PCR according to procedures in ref *27*. The resulting DNA fragment was cut with *Bpu*1102I and ligated into pETBlue-1 cut with *Eco*RV/*Bpu*1102I. The correct insertion was verified by DNA sequencing according to procedures in ref *28*, and the resulting plasmid was designated pETBlue-1/*nuoEF*$_{Strep}$*G*. A scheme for the construction of the expression vectors is depicted in Figure 1.

Since the *Strep* tag II is suspected of interfering with crystallization (*29*), a 6×His tag was also engineered to subunit NuoF. For the exchange of the *Strep* tag II sequence with the 6×His tag sequence, part of the genes *nuoF* and *nuoG* were amplified with the plasmid serving as template. Using primers Pe (5′-GAT AAT AAT AGA GAG GGA TCC CCA CC-3′), which carries the intrinsic *Bam*HI site of *nuoF* (underlined), and Pf (5′-*ATG ATG ATG ATG ATG ATG TCC GGC* AAG GGG AAG GGA AGC AGA TTT CTT TC-3′) carrying the inverted 6×His tag sequence including two spacer amino acids (italics), we amplified *nuoF′*. The

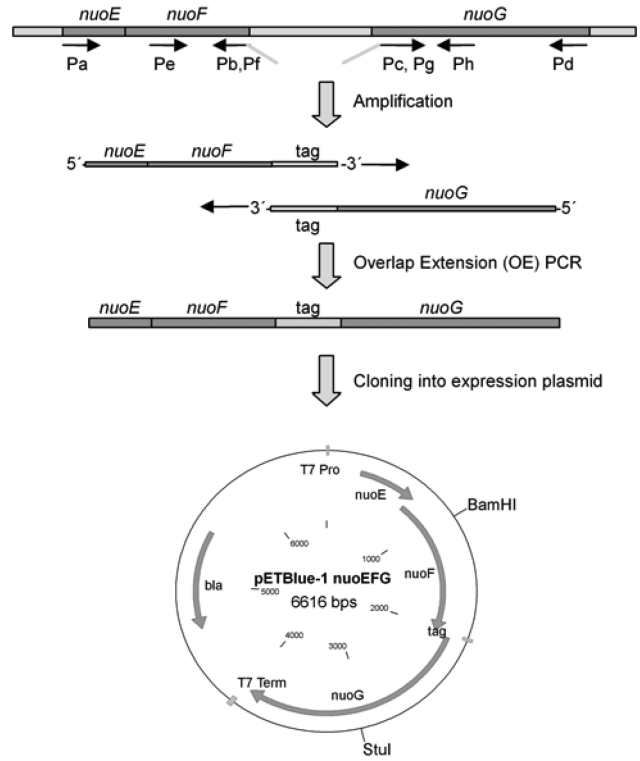

FIGURE 1: Cloning scheme of the expression plasmids pETBlue-1/*nuoEF*$_{tag}$*G*. A tag sequence was inserted between *nuoF* and *nuoG*. The sequences of the *Strep* tag II and the 6×His tag are shown in gray. Primers Pb and Pf as well as Pc and Pg are identical except for the sequence regions coding for the different tags. Restriction sites for *Bam*HI and *Eco*147I (*Stu*I) are indicated in the map of the expression plasmid.

gene *nuoG′* was amplified from primers Pg (5′-*GCC GGA CAT CAT CAT CAT CAT CAT* TAA AAT CGA ATT CAA GGA GGT TGA TAT GTC C-3′) carrying the 6×His tag sequence including two spacer amino acids (italics) and Ph (5′-CTG AGA GGC CTT TGC TAT CCT TAA AAC-3′) carrying the intrinsic *Eco*147I site of *nuoG* (underlined). Both amplicons were subjected to an OE-PCR as described above. The resulting DNA fragment was cut with *Bam*HI/*Eco*147I and ligated into the *Bam*HI/*Eco*147I sites of pETBlue-1/*nuoEF*$_{Strep}$*G*. The correct insertion was verified by DNA sequencing, and the resulting plasmid was designated pETBlue-1/*nuoEF*$_{His}$*G* (Figure 1).

Heterologous Expression of the nuo Genes. Competent cells of strain *E. coli* Rosetta(DE3)pLacI were transformed either with expression plasmid pETBlue-1/*nuoEF*$_{Strep}$*G* or with pETBlue-1/*nuoEF*$_{His}$*G*. Transformants were grown in a 10 L culture of LB medium with 1% glucose and were induced by an addition of 1 mM isopropyl-β-D-thiogalactopyranoside after the cells reached an optical density of approximately 0.8 at 600 nm. Cells were grown until entering the stationary phase and harvested by flow-through centrifugation. The sediment was washed with 50 mM MOPS/NaOH, 50 mM NaCl, pH 7.0, and stored at −80 °C.

Preparation of the Cytoplasmic Fraction. Approximately 12 g of cells (wet weight) containing NuoF engineered with a 6×His tag was resuspended in 20 mL of 50 mM MOPS/NaOH, 200 mM NaCl, 20 mM imidazole, and 30 μM phenylmethanesulfonyl fluoride (PMSF), pH 7.0, and disrupted by passing through a French pressure cell (SLM Aminco) twice at 110 MPa. The suspension was centrifuged at 184 000*g* (Optima LE-80K ultracentrifuge, type 70.1 Ti

rotor, Beckman Coulter, 50 000 rpm, 4 °C) for 1 h. The supernatant was treated as a cytoplasmic fraction. For purification of the protein engineered with the *Strep* tag II, 12 g of cells was resuspended in 20 mL of 50 mM MOPS/NaOH, 200 mM NaCl, 30 μM PMSF, pH 7.0, and treated as described above. Avidin (Sigma, 20 μg per gram of cells) was added to the cytoplasmic fraction.

Purification of the NuoEF Subcomplex. The procedure for purifying the 6×His-tagged NuoEF subcomplex is exemplarily described. Identical purification steps were performed when working with the protein engineered with the *Strep* tag II, with the exception of the use of appropriate *Strep*-tactin material for affinity chromatography. The results obtained with the *Strep* tag II modified protein were virtually identical to those obtained with the His-tagged protein.

The cytoplasmic fraction from approximately 12 g of cells was applied to a 10 mL Probond column (16 mm × 50 mm, Invitrogen, Carlsbad, CA) equilibrated in 50 mM MOPS/NaOH, 200 mM NaCl, 20 mM imidazole, 30 μM PMSF, pH 7.0, at a flow rate of 1.5 mL/min. The column was washed with the buffer containing 100 mM imidazole, and bound proteins were eluted using a 40 mL linear gradient from 100 to 500 mM imidazole at the same flow rate. Fractions with NADH/ferricyanide oxidoreductase activity were pooled, concentrated to 300 μL by ultrafiltration (Vivaspin 15, MWCO 30 000, Sartorius) and applied to a 109 mL TSKgel G4000SW column (21.5 mm × 30 cm, Tosoh) equilibrated in 50 mM MOPS/NaOH, 50 mM NaCl, 30 μM PMSF, pH 7.0, at a flow rate of 2.5 mL/min. Proteins were eluted in the same buffer at the same flow rate. Fractions with NADH/ferricyanide oxidoreductase activity were pooled and subjected to ion-exchange chromatography on a 5 mL Source15Q column (16 mm × 25 mm, GE Healthcare, München, Germany) equilibrated in the same buffer at a flow rate of 1.5 mL/min. Proteins were eluted with a 25 mL linear gradient from 50 to 350 mM NaCl in the same buffer. Fractions with NADH/ferricyanide oxidoreductase activity were pooled, concentrated to approximately 200 μL, and stored at −80 °C until further use.

For purification of the protein engineered with the *Strep* tag II, the cytoplasmic fraction was applied to a 13 mL *Strep*Tactin column (16 mm × 65 mm, IBA, Göttingen, Germany) equilibrated with 50 mM MOPS/NaOH, 200 mM NaCl, 30 μM PMSF, pH 7.0, at a flow rate of 0.8 mL/min and washed with the same buffer until the absorbance of the eluate at 280 nm reached its original value. Bound protein was eluted by applying the buffer with 2.5 mM desthiobiotin. Fractions with NADH/ferricyanide oxidoreductase activity were pooled and processed further by size-exclusion chromatography and ion-exchange chromatography as described above for the purification of the His-tagged protein.

EPR Spectroscopy. For EPR spectroscopy of the purified protein, 300 μL samples with a concentration of approximately 5 mg/mL were used. The samples were reduced by addition of a 1000-fold molar excess NADH and a few grains of dithionite. Aliquots of the cytoplasmic fraction were either treated with 15 mM NADH or the same volume of buffer. EPR spectra were recorded with an EMX 6/1 X-band spectrometer (Bruker, Karlsruhe, Germany) equipped with an ESR-9 helium-flow cryostat (Oxford Instruments, Wiesbaden, Germany). The magnetic field was calibrated using a strong or a weak pitch standard. The spectra were simulated as described previously (*30, 31*).

Electrochemistry. The ultrathin layer spectroelectrochemical cell with the cell path length set to 6−8 μm for UV/vis spectroscopy was used as previously described (*32*). UV/vis spectra were recorded in the range from 200 to 800 nm using a Cary 300 spectrometer (Varian, Palo Alto, CA). To avoid protein denaturation, the gold grid working electrode was chemically modified by a solution containing 2 mM cysteamine and 2 mM mercaptopropionic acid in a 1:1 ratio (*33*). In order to accelerate the redox reaction, the following mediators were used at a final concentration of 45 μM each (midpoint potential in brackets): ferrocenyltrimethylammoniumiodide (+643 mV), 1,1′-dicarboxylferrocene (+642 mV), diethyl-3-methylparaphenylenediamine (+365 mV), ferricyanide (+422 mV), dimethylparaphenylenediamine (+369 mV), 1,1′-dimethylferrocene (+339 mV), tetramethylparaphenylenediamine (+268 mV), tetrachlorobenzoquinone (+278 mV), 2,6-dichlorophenolindophenol (+215 mV), ruthenium hexamine chloride (+198 mV), 1,2-naphthoquinone (−143 mV), trimethylhydroquinone (+98 mV), menadione (−14 mV), 2-hydroxy-1,4-naphtoquinone (−127 mV), anthraquinone-2-sulfonate (−227 mV), neutral red (−309 mV), benzyl viologen (−362 mV), and methyl viologen (−448 mV). At the given concentrations and with the path length below 10 μm, no spectral contributions from the mediators in the UV/vis range used were detected in control experiments with samples lacking the protein. Approximately 6−7 μL of the protein solution were sufficient to fill the spectroelectrochemical cell. Potentials quoted with the data refer to the SHE′ (pH 7) potentials.

Crystallization. Aliquots of the preparation were used for crystallization attempts in a robotic system at the EMBL outstation, Hamburg, Germany, using 200 nL drops. The screening was performed with the following crystallization kits: Crystal Screen HT and Natrix HTX (both Hampton Research), JBScreens No. 1 to 10 (Jena Bioscience), and the Wizard Screens I and II (Emerald BioStructures). Three out of the 560 conditions tested led to the formation of crystals. Scaling up to 20 μL drops prepared manually led to growth of crystals using 0.1 M Tris/HCl, pH 7.0, 0.2 M NaCl, and 1.0 M sodium citrate as precipitant. The final protein concentration was 6 mg/mL.

Other Analytical Procedures. Protein concentrations were determined according to Bradford (*34*) for crude samples or fluorometrically using a Qubit fluorometer (Invitrogen, Carlsbad, CA). UV/vis spectra were recorded with a TIDAS II diode array spectrometer (J&M, Aalen, Germany) at room temperature. SDS−PAGE was performed according to Laemmli (*35*). Dynamic light scattering was performed with 15 μL of a 0.5 mg/mL protein solution in 50 mM MOPS/NaOH, 50 mM NaCl, pH 7.0, and a DynaPro-801 dynamic light scattering instrument (Protein Solutions, Charlottesville, VA). Twenty scans were recorded at room temperature, using a wavelength of 834 nm. Data were analyzed using the DynaPro-801 software (Protein Solutions, Santa Barbara, CA). Non-heme iron was determined as described (*36*). The flavin content was determined according to Koziol (*37*). The NADH/ferricyanide reductase activity was measured as described (*38*). Following SDS−PAGE, protein bands were either stained with Coomassie Blue or electroblotted onto 0.2 μm pore size PVDF membrane (Whatman plc, Kent, UK)

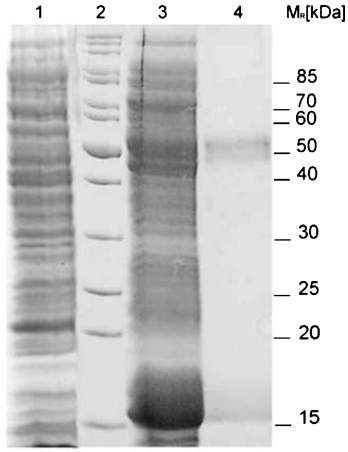

FIGURE 2: Coomassie-stained SDS gel of the cytoplasmic fraction of induced Rosetta(DE3)/pLacI/pETBlue-1 cells (lane 1), induced Rosetta(DE3)/pLacI/pETBlue-1/*nuoEF*$_{His}$*G* cells before (lane 3) and after incubation for 1 h at 80 °C (lane 4). Lane 2 shows the bands of molecular weight marker proteins. Their apparent molecular masses are indicated on the right.

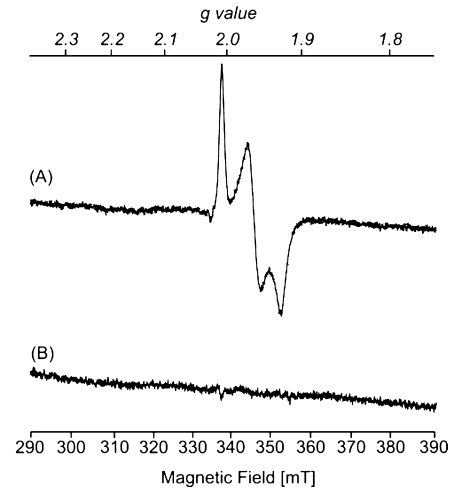

FIGURE 3: EPR redox difference spectra of the cytoplasmic fraction of induced cells of strain Rosetta(DE3)/pLacI/pETBlue-1/*nuoEF*$_{His}$*G* at 40 K. The NADH-reduced minus air-oxidized difference spectrum shows the signal of a binuclear Fe−S cluster, assigned to cluster N1a (A). The signal was completely lost after heating the cytoplasmic fraction for 1 h at 65 °C (B). Other EPR conditions were as follows: microwave power, 5 mW; microwave frequency, 9.462 GHz; modulation amplitude, 0.6 mT; time constant, 164 ms.

according to procedures in ref *39*. Proteins were N-terminally sequenced by automated Edman degradation (*40*) on a 477A Protein Sequencer with a 120A analyzer (Applied Biosystems, Foster City, CA).

RESULTS

Heterologous Overproduction of the Nuo Proteins. Cytoplasmic proteins from strain Rosetta(DE3)pLacI/pETBlue-1/*nuoEF*$_{His}$*G* were analyzed by SDS−PAGE. Compared with the cytoplasmic fraction of the induced strain carrying the plasmid without the insert, one band with a strongly enhanced intensity corresponding to a protein with an apparent molecular mass of approximately 16 kDa was clearly visible (Figure 2). An aliquot of the cytoplasm was incubated for 1 h at 80 °C, and denaturated proteins were removed by centrifugation for 1 min at 13 200*g*. The heat-treated sample was subjected to SDS−PAGE revealing the presence of one protein with an apparent molecular mass of approximately 16 kDa, most likely corresponding to the one with enhanced intensity in the cytoplasmic fraction, and two proteins with a mass of approximately 50 kDa, which were hardly discernible (Figure 2). The proteins were blotted on a PVDF membrane, and their N-terminal sequences were determined. The N-terminus of the protein with an apparent molecular mass of 16 kDa (MFKTEFEFPE) was identical to that of *A. aeolicus* NuoE (M_r = 18.55 kDa) as derived from its DNA sequence (*19*). The N-terminus of each of the two proteins with an apparent molecular mass of approximately 50 kDa (MRSYPAIPRI) was identical to that of *A. aeolicus* NuoF (M_r = 47.51 kDa). The two bands assigned to NuoF may be the result either of different conformations of the protein or of a partial proteolysis at the C-terminus. We failed to detect NuoG in any of the samples.

For EPR spectroscopy, the cytoplasmic fraction of the expression strain was concentrated 5-fold. One aliquot was reduced by addition of NADH; another aliquot was diluted with the same volume of buffer. EPR spectra from both samples were recorded at 40 K. The spectrum of the oxidized sample was subtracted from the spectrum of the NADH-reduced sample showing an intense signal of a binuclear Fe−S cluster with rhombic symmetry (Figure 3). The *g*-values of the signal were determined to be $g_{x,y,z}$ = 1.923, 1.97, and 2.005, respectively. These *g*-values are very similar to those obtained from the Fe−S cluster N1a of the *E. coli* complex I (see Table 2; *24, 31, 41*). Because of this and its shape, the signal was tentatively assigned to cluster N1a of the A. aeolicus complex I located on NuoE. Incubation of the cytoplasmic fraction for 1 h at 65 °C led to a complete loss of the signal (Figure 3) indicating that NuoE loses its cofactor under these conditions, although the protein itself is not aggregated at this temperature (Figure 2). Thus, heating the sample is not a method of choice in the separation of the thermostable *A. aeolicus* Nuo proteins from the proteins of the *E. coli* host. Signals that were unambiguously assigned to the tetranuclear cluster N3 expected to be present in the overproduced NuoF were not observed in the EPR difference spectrum recorded at 13 K due to the presence of multiple signals (data not shown). Identical results were obtained with the cytoplasmic fraction from strain Rosetta(DE3)pLacI/pETBlue-1/*nuoEF*$_{Strep}$*G*.

Purification of the NuoEF Subcomplex. The NuoEF subcomplex of the *A. aeolicus* complex I engineered with a His tag was purified to homogeneity by means of affinity chromatography on Ni^{2+}-IDA, size exclusion chromatography on TSKgel G4000SW, and ion-exchange chromatography on Source15Q. The protein eluted from the Ni^{2+}-IDA material at 390 mM imidazole, from the Source15Q material column at 250 mM NaCl, and at an elution volume of approximately 90 mL from the TSK column (Figure 4). From 12 g of cells (wet weight) routinely 5 mg of the NuoEF subcomplex were obtained (Table 1). The last purification step was necessary to remove a contamination with an apparent molecular mass of approximately 30 kDa although it led to a decrease of the specific activity (Table 1). SDS−PAGE analysis showed no impurities after the final anion-exchange chromatography (Figure 4). A sharp band corresponding to a protein with an apparent molecular mass of approximately 50 kDa and a broad band corresponding

Table 1: Isolation of the *A. aeolicus* NuoEF Subcomplex from 12 g of Cells of Strain Rosetta(DE3)/pLacI/*nuoEF*$_{His}$*G*

preparation	volume [mL]	protein [mg]	NADH/ferricyanide oxidoreductase activity: total [μmol min^{-1}]	NADH/ferricyanide oxidoreductase activity: specific [μmol min^{-1} mg^{-1}]	yield [%]
cytoplasm	32	520	3420	7	100
Probond Ni^{2+}-IDA	15	50	1530	31	45
TSKgel G4000SW	20	10	550	55	16
Source15Q	3	5	240	48	7

Table 2: Properties of Fe−S Clusters N1a and N3 from *A. aeolicus* (This Work) and *E. coli* (*31*)

cluster	organism	*g*-values ($g_{x,y,z}$)	linewidth ($L_{x,y,z}$) [mT]	midpoint potential [mV]
N1a [2Fe−2S]	*A. aeolicus*	1.92; 1.97; 2.01	0.9; 1.1; 0.8	−254
	E. coli	1.92; 1.95; 2.00	0.8; 0.95; 0.6	−250
N3 [4Fe−4S]	*A. aeolicus*	1.88; 1.95; 2.047	1.8; 2.0; 3.5	−164
	E. coli	1.88; 1.94; 2.045	1.9; 1.5; 1.4	−270

to a 16 kDa protein were detected. The proteins were blotted onto a PVDF membrane and identified by N-terminal sequencing as described above. The N-terminus of the 16 kDa protein revealed its identity as NuoE, that of the 50 kDa protein as NuoF (see above). The broad band from NuoE might have derived from its partial digestion. To test this possibility, the mass of the proteins was determined by means of electron spray ionization mass spectrometry (Supporting Information, Figure S1). The mass of NuoE and NuoF as deduced from their DNA sequences is 18 550.6 and 48 724.8 Da. The experimentally determined mass of 18 545.0 and 48 708.0 Da was in good agreement with the expected values. The small differences of 5.6 and 16.8 Da, respectively, indicate either modifications of the proteins or, more likely, deviations from the amino acid composition deduced from the DNA sequence. However, no additional band was detected on a silver-stained gel with an N-terminal sequence corresponding to protein derived from proteolytic cleavage of one of the *A. aeolicus* Nuo proteins (data not shown). In addition, the *E. coli* NuoE and NuoF were neither detected in the preparation by N-terminal sequencing nor by mass spectrometry, although the strain used for overproduction contains the *E. coli nuo* genes. Possibly formed chimeras of both bacterial proteins containing the *E. coli* NuoF are not expected to be purified using affinity chromatography.

The NuoEF subcomplex engineered with the *Strep* tag II sequence was purified by an identical protocol but using *Strep*Tactin as chromatography material in the first step, the affinity chromatography. Bound proteins were eluted in the presence of 2.5 mM desthiobiotin. With this procedure, one single elution peak was obtained (data not shown). Fractions with NADH/ferricyanide oxidoreductase activity still contained impurities as judged from SDS−PAGE. Therefore, the fractions were pooled and further processed as described above. The identity of the proteins was verified by N-terminal sequencing. This procedure yielded approximately 4 mg of protein of the same purity as obtained with the His-tagged protein.

Electron Transfer Activity. The NADH/ferricyanide oxidoreductase activity of both preparations was determined at various temperatures in a range from 25 to 90 °C. The enzymatic activity reached its optimum at 85 °C (Supporting Information, Figure S2), which is in accordance with the optimal growth temperature of *A. aeolicus* and the temperature of maximal complex I activity in the membrane (*21*). This activity is mediated by the FMN and independent of the presence of cluster N1a, which is lost at 65 °C (Figure 3). With decyl-ubiquinone as the acceptor, no activity was determined in the preparation.

Internal Redox Groups. The preparation should contain one FMN, the binuclear FeS cluster N1a, and the tetranuclear cluster N3 as deduced from the conserved sequence motifs and from the structure of the *T. thermophilus* homologues (*10, 12*). The specific FMN content of two independent preparations containing either the His tag or the *Strep* tag II sequence varied from 13 to 15 nmol/mg and the specific iron content from 80 to 95 nmol/mg. Use of the protein molecular mass of 67 kDa gives 0.9−1.0 mol of FMN and 5−6 mol of iron per mol of NuoEF subcomplex. Thus, all cofactors of the NuoEF subcomplex were present in the preparation in stoichiometric amounts.

The UV/vis spectrum of the preparation as isolated (Figure 5) showed an intense peak at 270 nm, which was assigned to the FMN (*42*). This signal overlaps strongly with the absorption of the aromatic amino acid residues at 280 nm. The absorption of the FMN at 270 nm is visible in this subcomplex but not in the entire complex due to the high molar FMN content of the former. Absorption peaks of the FMN are also visible at 370 and 450 nm (*23, 42*). The absorption peaks at 330, 410, and 560 nm are attributed to the binuclear Fe−S cluster N1a (*43*). The broad shoulders around 375 and 410 nm indicated the presence of the tetranuclear Fe−S cluster N3 (*23, 43, 44*).

The preparation was reduced by an addition of dithionite, and the reoxidation of the sample by oxygen from the air was observed in a stirred cuvette by means of UV/vis diode array spectroscopy. The concentration of dithionite was measured at 315 nm. After the oxidation of the excess dithionite but not of the sample, a spectrum of the reduced preparation was recorded. The reduced-minus-oxidized UV/vis difference spectrum was calculated and indicated that the cofactors of the NuoEF subcomplex were redox active (Figure 5).

The nature of the Fe−S clusters was further investigated by means of EPR spectroscopy. The preparation was reduced by excess NADH and dithionite, and EPR spectra were recorded at 40 and 13 K (Figure 6). At 40 K and 2 mW microwave power, the signal of a binuclear Fe−S cluster was clearly visible. Simulation of the rhombic spectrum revealed the *g*-values ($g_{x,y,z}$ = 1.923, 1.972, and 2.012) similar

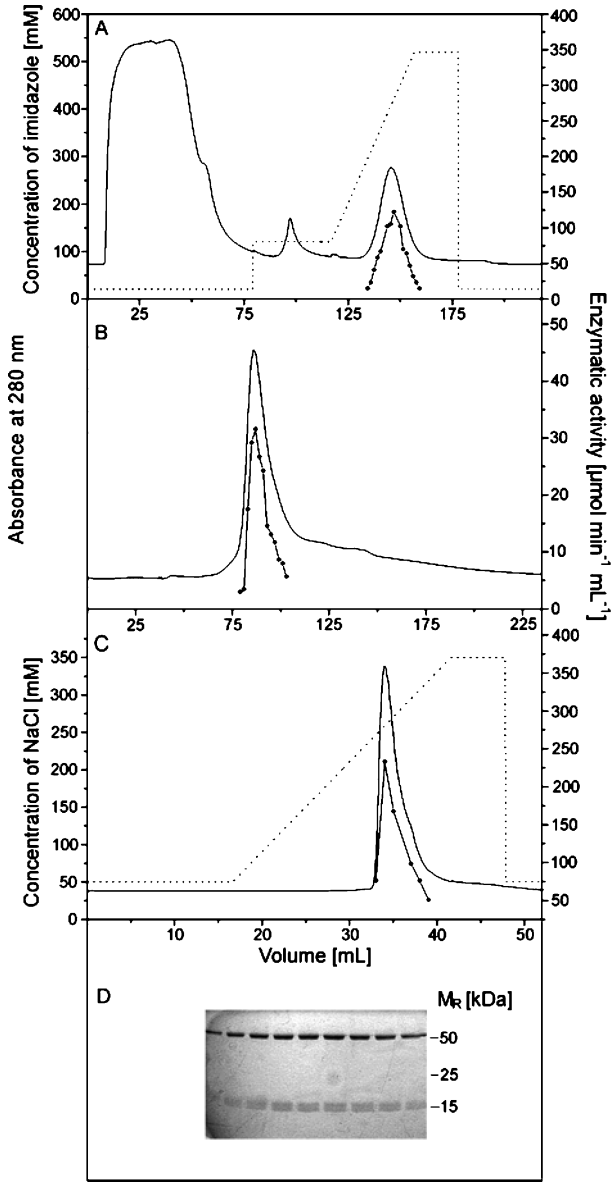

FIGURE 4: Isolation of the *A. aeolicus* NuoEF subcomplex overproduced in *E. coli*: chromatography on Ni^{2+}-IDA (A), TSKgel (B), and Source15Q (C) and (D) SDS−PAGE of the fractions with NADH/ferricyanide oxidoreductase activity; (—) absorbance at 280 nm; (◆) NADH/ferricyanide oxidoreductase activity; (•••) gradients. The numbers in panel D correspond to the apparent molecular masses $\times 10^{-3}$ Da.

to those observed in the EPR difference spectrum of the cytoplasmic fraction (Figure 3). According to the shape of the signal and the *g*-values, the EPR spectrum was attributed to cluster N1a located on subunit NuoE of the *A. aeolicus* complex I (Table 2). Contributions from another compound with *g*-values of 1.95 and 2.047 were detected. The spectrum of the preparation recorded at 13 K revealed that these signals derived from an additional, tetranuclear Fe−S cluster. The *g*-values of the rhombic signal were simulated as $g_x = 1.884$, $g_y = 1.947$, and $g_z = 2.047$ (Figure 6). They correspond well to those reported for the *E. coli* cluster N3 located on NuoF (Table 2). Thus, the signals detected at 13 K were attributed to cluster N3 of the *A. aeolicus* complex I. Because the signals from N3 were also detectable in the spectrum recorded at 40 K (see above), the *A. aeolicus* N3 in the NuoEF preparation exhibits a slower relaxation than that of

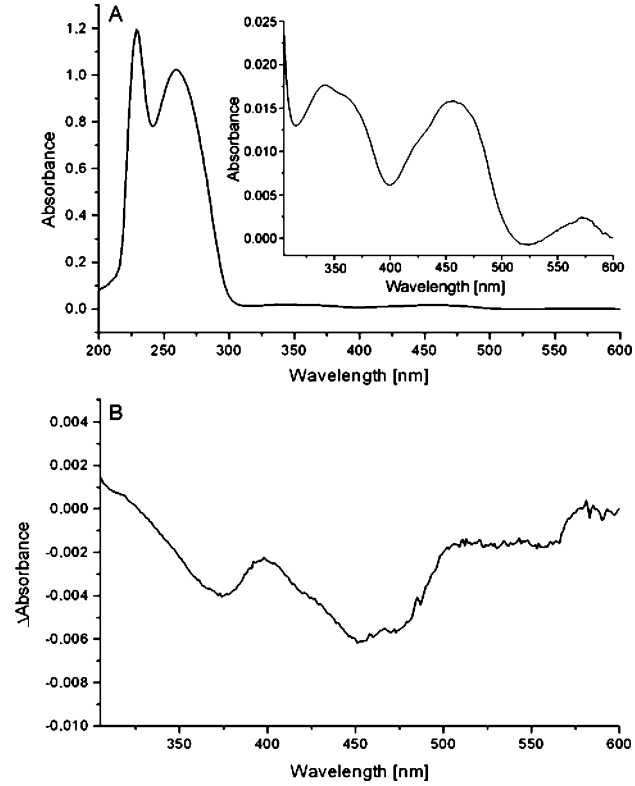

FIGURE 5: UV/vis spectra of the preparation. Panel A shows the spectrum of an air-oxidized sample (16 μM). The inset shows an enlarged view of the region from 300 to 600 nm. Absorption at 220, 270, 370, and 450 nm was assigned to the FMN, absorption at 330 and 560 nm to the binuclear Fe−S cluster N1a, and the broad shoulder around 410 nm to the tetranuclear Fe−S cluster N3. Panel B shows the dithionite-reduced minus air-oxidized difference spectrum of the preparation (see text for details).

the entire *E. coli* complex. No signals were detectable in the oxidized sample.

To determine the midpoint potential of the cofactors, an electrochemical titration was performed as described previously (*33*). The preparation was concentrated to 35 mg/mL, and mediators were added (*32*). The UV/vis spectra of the preparation were recorded at distinct midpoint potentials from −500 to 0 mV after equilibration of the sample in steps of 20−40 mV. The data were fitted to a Nernst equation, and three midpoint potentials were identified (Supporting Information, Figure S3). The redox group with a midpoint potential of −330 mV showing an $n = 2$ transition was attributed to the FMN; the two groups with an $n = 1$ transition and a midpoint potential of −250 and −160 mV were attributed to Fe−S clusters N1a and N3, respectively. In this work, we determined the midpoint potential of the FMN in the isolated *E. coli* complex I to −320 mV, which is in very good agreement with that of the FMN in the *A. aeolicus* NuoEF subcomplex. The midpoint potential of the *A. aeolicus* cluster N1a is close to that previously determined for the isolated *E. coli* complex I (Table 2). However, the midpoint potential of N3 is approximately 100 mV higher than that of the *E. coli* N3 (Table 2). Either the potential of the *A. aeolicus* N3 significantly differs from that of the *E. coli* complex I by nature or the midpoint potential of the *A. aeolicus* N3 is shifted to a higher value due to the lack of subunit NuoG in the NuoEF subcomplex. NuoG is in close contact with NuoF at the site where N3 is bound (*10*).

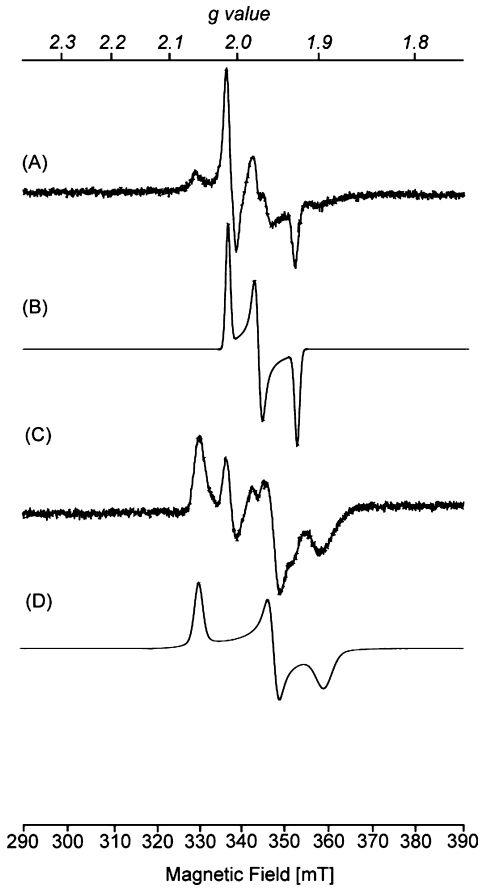

FIGURE 6: EPR spectra of the preparation. The samples were reduced by NADH and dithionite, and spectra were recorded at 40 K and 2 mW (A) and at 13 K and 5 mW (C). The other EPR conditions were the same as indicated in Figure 3. Spectrum B shows a simulation of spectrum A using the follwing parameters: $g_{x,y,z}$ = 1.922, 1.971, and 2.005; $L_{x,y,z}$ = 0.9, 1.1, and 0.8 mT. Spectrum D shows a simulation of spectrum C using the follwing parameters: $g_{x,y,z}$ = 1.884, 1.947, and 2.047; $L_{x,y,z}$ = 0.9, 1.1, and 0.8 mT.

Homogeneity of the Preparation. The homogeneity of the preparation was analyzed by DLS. An average of 20 measurements revealed the presence of one population with a hydrodynamic radius of 3.50 nm corresponding to a molecular mass of approximately 62 kDa. This deviates by 7% from the molecular mass of the NuoEF subcomplex monomer of 67 kDa as derived from the DNA sequence.

The structural integrity of the preparations was examined by analytical gel filtration on a TSKgel G4000SW column. The elution profile of the preparations with both modifications showed a single homogeneous peak eluting at 92 mL with a slight end-tailing (Supporting Information, Figure S4). These data demonstrate the structural integrity and homogeneity of both preparations.

Crystallization of the Preparation. The high-throughput crystallization trial at the EMBL outstation, Hamburg, using a robotic system and a 200 nL setup led to the identification of three conditions leading to the crystallization of the sample equipped with a His tag. Due to this, we did not try to crystallize the Strep-tagged version of the preparation. Using the hanging drop technique and manually prepared 20 μL drops, we obtained crystals of 600 × 200 μm^2 size using 0.1 M Tris/HCl pH 7.0, 0.2 M NaCl, and 1.0 M sodium citrate as precipitant (Figure 7). The crystals diffracted more than 2 Å revealing a space group of $P2_12_12_1$ (a = 63 Å, b = 117 Å, c = 190 Å and $\alpha = \beta = \gamma = 90°$).

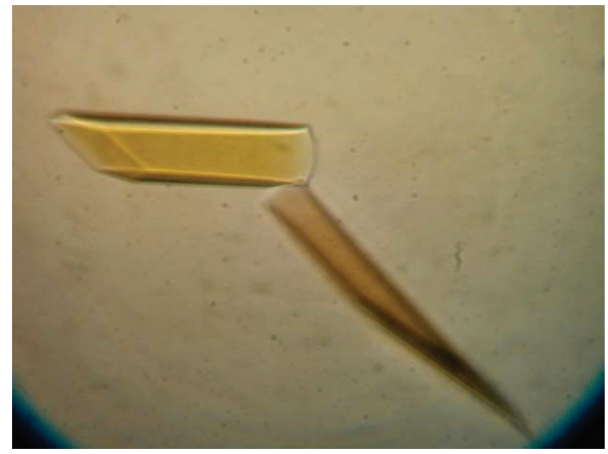

FIGURE 7: Crystal of the preparation of the *A. aeolicus* NuoEF subcomplex heterologously overproduced in *E. coli*.

DISCUSSION

In this work, we report the heterologous overproduction and isolation of the NuoEF subcomplex of the *A. aeolicus* complex I in *E. coli*. The expression vector contained the genes *nuoE*, *nuoF*, and *nuoG* coding for the three subunits comprising the NADH dehydrogenase fragment of the complex (*23, 24, 45*). However, only NuoE and NuoF were detectable after the induction of expression. In contrast, overexpression of the *E. coli nuoE*, *nuoF*, and *nuoG* under the control of the same promoter led to the production of the individual subunits as inclusion bodies (*23*). We were not able to detect the *A. aeolicus* NuoG in whole cells, in the cytoplasmic fraction, in the fraction containing inclusion bodies, or in the membrane fraction. However, placing the *A. aeolicus nuoG* directly downstream of the T7 promotor led to the production of NuoG as inclusion bodies. The identity of NuoG was confirmed by N-terminal sequencing (data not shown). Unlike in *E. coli*, *nuoE*, *nuoF*, and *nuoG* are not clustered on the *A. aeolicus* chromosome. Therefore, two successive cloning steps were necessary to insert the genes into the expression plasmid, thereby building an artificial intergenic region between *nuoF* and *nuoG* (Figure 1). No sites for transcriptional or translational termination were identified within this region, but the artificial intergenic region is suspected of interfering with the expression of *nuoG*. Currently, we are trying to replace the artificial region with the native *nuoF*/*nuoG* intergenic region of the *E. coli* chromosome.

The spreading of the genes on the *A. aeolicus* chromosome relates to the function of the corresponding proteins. Phylogenetic analysis revealed that a common progenitor of complex I present in all three domains of life contained all subunits with the exception of NuoE, NuoF, and NuoG comprising the NADH dehydrogenase fragment (*5, 12*). This ancestral complex was further equipped with subunit NuoG during evolution, giving rise to a binding site for a different electron donor (*11, 14*). The C-terminus of NuoG is homologous to molybdo-bis(molybdopterin-guanin-dinucleotide) (Mo-bisMGD) enzymes (*46*). This cofactor was lost in complex I during evolution, while an Fe−S cluster (named N7 in complex I) of the Mo-bisMGD enzymes was retained in some species for structural reasons (*47, 48*). The N-terminal part of NuoG is homologous to FeFe-hydrogenases, which contain Fe−S clusters homologous to N1b, N4, and

N5 (*46*). The distance between these clusters and N7 is too large for a physiological electron transfer (*14, 49*). FeFe-hydrogenases contain an additional Fe−S cluster named FS4A, which has no homologue in complex I (*11, 14, 50*). In contrast to the other *nuoG* sequences, that of *A. aeolicus* codes for cysteines that might ligate a complex I homologue of cluster FS4A. Thus, the *A. aeolicus* NuoG may harbor an additional Fe−S cluster connecting N7 with the electron pathway to the quinone reduction site (*11, 14*). Later acquisition of NuoE and NuoF led to the emergence of the present complex I and enabled the use of NADH as substrate. Through this acquisition, the Fe−S clusters of the electron pathway to the substrate binding site on NuoG were superfluous. Thus, the subsequent acquisition of NuoG on the one hand and NuoEF on the other hand might be reflected in the different chromosomal localization of *nuoG* and *nuoEF*.

Homologues of NuoE and NuoF are also found in hydrogenosomes, double-membraned organelles of diverse unicellular anaerobic eukaryotes that produce ATP and hydrogen (*51*−*54*). It was shown that the hydrogenosomal homologues of NuoE and NuoF are present in a NuoEF subcomplex and that this subcomplex is fused to a hydrogenase enabling the direct regeneration of NAD^+ coupled with the reduction of protons to hydrogen. It is believed that the genes of the hydrogenosomal polyprotein were acquired by lateral gene transfer (*51*−*54*).

The NuoEF subcomplex was also obtained by expressing the orthologues from *Paracoccus denitrificans* named *nqo2* and *nqo1*, respectively, heterologously in *E. coli* using two plasmids (*55*). The preparation contained a [2Fe−2S] cluster in nearly stoichiometric amounts but neither the FMN nor the [4Fe−4S] cluster (*55*). After reconstitution *in vitro* under anaerobic conditions, the preparation contained approximately 0.5 mol of FMN and 0.5 mol of [4Fe−4S] cluster per mol of protein (*55*). In our study, the NuoEF subcomplex expressed from one plasmid contained the cofactors in stoichiometric amounts after purification. This might be because the *A. aeolicus* proteins show a higher degree of sequence similarity to the *E. coli* orthologues than to those from *P. denitrificans*, which possibly enables their recognition as substrates for the *E. coli* proteins involved in cofactor insertion. As the reconstituted NuoEF subcomplex from *P. denitrificans*, our preparation exhibited high turnover with soluble electron acceptors (*55*).

The UV/vis spectrum of the *A. aeolicus* subcomplex is in good agreement with that of the isolated and reconstituted *P. denitrificans* subcomplex. It is indicative of the presence of the flavin and the Fe−S clusters (Figure 5). The UV/vis (reduced-minus-oxidized) difference spectrum (Figure 6) reveals that all cofactors are redox-active. By means of the respective EPR spectroscopic characteristics and the midpoint potentials, the [2Fe−2S] cluster was attributed to N1a and the [4Fe−4S] cluster to N3. This assignment is in agreement with data obtained by site-directed mutagenesis (*56, 57*) and structural studies (*10*). The *g*-values and line width of N1a and N3 of the *A. aeolicus* complex I are very similar to those of the *E. coli* complex (Table 2) but differ from those of other bacterial sources (*58*).

Despite the fact that the *A. aeolicus* NuoEF subcomplex was thermostable and exhibited an optimal turnover at 85 °C (Supporting Information, Figure S3), N1a was lost after incubation at 65 °C for 1 h (Figure 3). At this temperature, the *E. coli* proteins denature, a feature used to separate overproduced *A. aeolicus* proteins from host proteins (*59*). The *A. aeolicus* [2Fe−2S] ferredoxin AaFd4, which is homologous to the C-terminal domain of NuoE, was purified by a procedure containing the denaturing step without losing the Fe−S cluster (*60*). However, the complex structure of the NuoEF subcomplex might prohibit such a simple purification step. Therefore, the NuoEF subcomplex was individually engineered with a 6×His tag and a *Strep* tag II at the same position of NuoF and purified by affinity chromatography. Both purification methods led to a similar purity of the subcomplex, but the yield of the preparation of the His-tagged variant was slightly higher. The different tags influenced neither the assembly of the subcomplex nor its equipment with the cofactors nor the stability of the preparation. However, two additional chromatographic steps were necessary to obtain a pure and monodisperse preparation of both protein variants as judged from SDS−PAGE and analytical size-exclusion chromatography.

The variant engineered with the His tag was crystallized, and the crystals diffracted higher than 2 Å. Further work to resolve the phase problem and to obtain a structural model is in progress.

ACKNOWLEDGMENT

We thank Dr. Jürgen Wörth for mass spectrometry experiments and Linda Williams for her help in correcting the manuscript.

SUPPORTING INFORMATION AVAILABLE

The mass spectra of the NuoEF preparation, temperature dependence of the enzymatic activity of the preparation, redox titration of the cofactors, and the analytical gel filtration of the preparation. This material is available free of charge via the Internet at http://pubs.acs.org.

REFERENCES

1. Weiss, H., Friedrich, T., Hofhaus, G., and Preis, D. (1991) The respiratory-chain NADH dehydrogenase (complex I) of mitochondria. *Eur. J. Biochem. 197*, 563–576.
2. Walker, J. E. (1992) The NADH:ubiquinone oxidoreductase (complex I) of respiratory chains. *Q. Rev. Biophys. 25*, 253–324.
3. Ohnishi, T. (1998) Iron-sulfur clusters/semiquinones in complex I. *Biochim. Biophys. Acta 1364*, 186–206.
4. Carroll, J., Fearnley, I. M., Skehel, J. M., Shannon, R. J., Hirst, J., and Walker, J. E. (2006) Bovine complex I is a complex of 45 different subunits. *J. Biol. Chem. 281*, 32724–32727.
5. Friedrich, T., Steinmüller, K., and Weiss, H. (1995) The proton-pumping respiratory complex I of bacteria and mitochondria and its homologue in chloroplasts. *FEBS Lett. 367*, 107–111.
6. Grigorieff, N. (1998) Three-dimensional structure of bovine NADH: ubiquinone oxidoreductase (complex I) at 22 Å in ice. *J. Mol. Biol. 277*, 1033–1046.
7. Böttcher, B., Scheide, D., Hesterberg, M., Nagel-Steger, L., and Friedrich, T. (2002) A novel, enzymatically active conformation of the *Escherichia coli* NADH:ubiquinone oxidoreductase (complex I). *J. Biol. Chem. 277*, 17970–17977.
8. Baranova, E. A., Holt, P. J., and Sazanov, L. A. (2007) Projection structure of the membrane domain of *Escherichia coli* respiratory complex I at 8 Å resolution. *J. Mol. Biol. 366*, 140–154.
9. Yagi, T., and Matsuno-Yagi, A. (2003) The proton-translocating NADH-quinone oxidoreductase in the respiratory chain: The secret unlocked. *Biochemistry 42*, 2266–2274.
10. Sazanov, L. A., and Hinchliffe, P. (2006) Structure of the hydrophilic domain of respiratory complex I from *Thermus thermophilus*. *Science 311*, 1430–1436.

11. Friedrich, T., and Pohl, T. (2007) NADH as Donor, in *EcoSal - Escherichia coli and Salmonella: Cellular and Molecular Biology* (Böck, A., Curtis, R., III., Kaper, J. B., Neidhardt, F. C., Nyström, T., Slauch, J. M., and Squires, C. L., Eds.), Chapter 3.2.4., ASM Press, Washington D.C., http://www.ecosal.org.
12. Friedrich, T., and Scheide, D. (2000) The respiratory complex I of bacteria, archaea and eukarya and its module common with membrane-bound multisubunit hydrogenases. *FEBS Lett. 479*, 1–5.
13. Brandt, U., Kerscher, S., Dröse, S., Zwicker, K., and Zickermann, V. (2003) Proton pumping by NADH:ubiquinone oxidoreductase. A redox driven conformational change mechanism? *FEBS Lett. 545*, 9–17.
14. Sazanov, L. A. (2007) Respiratory complex I: Mechanistic and structural insights provided by the crystal structure of the hydrophilic domain. *Biochemistry 46*, 2275–2288.
15. Ohnishi, T., and Salerno, J. C. (2005) Conformation-driven and semiquinone-gated proton-pump mechanism in the NADH-ubiquinone oxidoreductase (complex I). *FEBS Lett. 579*, 4555–4561.
16. Huber, R., Wilharm, T., Huber, D., Trincone, A., Burggraf, S., König, H., Rachel, R., Rockinger, I., Fricke, H., and Stetter, K. O. (1992) *Aquifex pyrophilus* gen. nov. sp. nov., represents a novel group of marine hyperthermophilic hydrogen-oxidizing bacteria. *Syst. Appl. Microbiol.* 340–351.
17. Burggraf, S., Olsen, G. J., Stetter, K. O., and Woese, C. R. (1992) A phylogenetic analysis of Aquifex pyrophilus. *Syst. Appl. Microbiol.* 352–356.
18. Pitulle, C., Yang, Y., Marchiani, M., Moore, E. R., Siefert, J. L., Aragno, M., Jurtshuk, P., Jr., and Fox, G. E. (1994) Phylogenetic position of the genus *Hydrogenobacter*. *Int. J. Syst. Bacteriol.* 620–626.
19. Deckert, G., Warren, P. V., Gaasterland, T., Young, W. G., Lenox, A. L., Graham, D. E., Overbeek, R., Snead, M. A., Keller, M., Aujay, M., Huber, R., Feldman, R. A., Short, J. M., Olsen, G. J., and Swanson, R. V. (1998) The complete genome of the hyperthermophilic bacterium *Aquifex aeolicus*. *Nature 392*, 353–358.
20. Friedrich, T. (1998) The NADH:ubiquinone oxidoreductase (complex I) from *Escherichia coli*. *Biochim. Biophys. Acta 1364*, 134–146.
21. Scheide, D., Huber, R., and Friedrich, T. (2002) The proton-pumping NADH:ubiquinone oxidoreductase (complex I) of *Aquifex aeolicus*. *FEBS Lett. 512*, 80–84.
22. Peng, G., Fritzsch, G., Zickermann, V., Schägger, H., Mentele, R., Lottspeich, F., Bostina, M., Radermacher, M., Huber, R., Stetter, K. O., and Michel, H. (2003) Isolation, characterization and electron microscopic single particle analysis of the NADH:ubiquinone oxidoreductase (complex I) from the hyperthermophilic eubacterium *Aquifex aeolicus*. *Biochemistry 42*, 3032–3039.
23. Braun, M., Bungert, S., and Friedrich, T. (1998) Characterization of the overproduced NADH dehydrogenase fragment of the NADH: ubiquinone oxidoreductase (complex I) from *Escherichia coli*. *Biochemistry 37*, 1861–1867.
24. Uhlmann, M., and Friedrich, T. (2005) EPR signals assigned to Fe/S cluster N1c of the *Escherichia coli* NADH:ubiquinone oxidoreductase (complex I) derive from cluster N1a. *Biochemistry 44*, 1653–1658.
25. Hanahan, D. (1983) Studies on transformation of *Escherichia coli* with plasmids. *J. Mol. Biol. 166*, 557–580.
26. Sambrook, J., and Russell, D. W. (2001) *Molecular Cloning: A laboratory manual*, 3rd ed., Cold Spring Harbor Laboratory Press, New York.
27. Higuchi, R., Krummel, B., and Saiki, R. K. (1988) A general method of in vitro preparation and specific mutagenesis of DNA fragments: Study of protein and DNA interactions. *Nucleic Acids Res. 16*, 7351–7367.
28. Sanger, F., Nicklen, S., and Coulson, A. R. (1978) DNA sequencing with chain-terminating inhibitors. *Proc. Natl. Acad. Sci. U.S.A. 74*, 5463–5467.
29. Bucher, M. H., Evdokimov, A. G., and Waugh, D. S. (2002) Differential effects of short affinity tags on the crystallization of *Pyrococcus furiosus* maltodextrin-binding protein. *Acta Crystallogr. D58*, 392–397.
30. Wang, D. C., Meinhardt, S. W., Sackmann, U., Weiss, H., and Ohnishi, T. (1991) The iron-sulfur clusters in the two related forms of mitochondrial NADH: ubiquinone oxidoreductase made by *Neurospora crassa*. *Eur. J. Biochem. 197*, 257–264.
31. Leif, H., Sled, V. D., Ohnishi, T., Weiss, H., and Friedrich, T. (1995) Isolation and characterization of the proton-translocating NADH: ubiquinone oxidoreductase from *Escherichia coli*. *Eur. J. Biochem. 230*, 538–548.
32. Hellwig, P., Scheide, D., Bungert, S., Mäntele, W., and Friedrich, T. (2000) FT-IR spectroscopic characterization of NADH:ubiquinone oxidoreductase (complex I) from *Escherichia coli*: Oxidation of FeS cluster N2 is coupled with the protonation of an aspartate or glutamate side chain. *Biochemistry 39*, 10884–10891.
33. Hellwig, P., Behr, J., Ostermeier, C., Richter, O. M., Pfitzner, U., Odenwald, A., Ludwig, B., Michel, H., and Mäntele, W. (1998) Involvement of glutamic acid 278 in the redox reaction of the cytochrome c oxidase from *Paracoccus denitrificans* investigated by FTIR spectroscopy. *Biochemistry 37*, 7390–7399.
34. Bradford, M. M. (1976) A rapid and sensitive method for the quantitation of microgram quantities of protein utilizing the principle of protein-dye binding. *Anal. Biochem. 72*, 248–254.
35. Laemmli, U. K. (1970) Cleavage of structural proteins during the assembly of the head of bacteriophage T4. *Nature 227*, 680–685.
36. Fish, W. W. (1988) Rapid colorimetric micromethod for the quantitation of complexed iron in biological samples. *Methods Enzymol. 158*, 357–364.
37. Koziol, J. (1971) Fluorometric analyses of riboflavin and its coenzymes. *Methods Enzymol. 18*, 253–285.
38. Friedrich, T., Hofhaus, G., Ise, W., Nehls, U., Schmitz, B., and Weiss, H. (1989) A small isoform of NADH:ubiquinone oxidoreductase (complex I) without mitochondrially encoded subunits is made in chloramphenicol-treated *Neurospora crassa*. *Eur. J. Biochem. 180*, 173–180.
39. Towbin, H., Staehelin, T., and Gordon, J. (1979) Electrophoretic transfer of proteins from polyacrylamide gels to nitrocellulose sheets: procedure and some applications. *Proc. Natl. Acad. Sci. U.S.A. 76*, 4350–4354.
40. Niall, H. D. (1974) Automated Edman degradation: The protein sequenator. *Methods Enzymol. 27*, 942–1010.
41. Spehr, V., Schlitt, A., Scheide, D., Guénebaut, V., and Friedrich, T. (1999) Overexpression of the *Escherichia coli nuo*-operon and isolation of the overproduced NADH:ubiquinone oxidoreductase (complex I). *Biochemistry 38*, 16261–16267.
42. Zhao, T., Cruz, F., and Ferry, J. G. (2001) Iron-sulfur flavoprotein (Isf) from *Methanosarcina thermophila* is the prototype of a widely distributed family. *J. Bacteriol. 183*, 6225–6233.
43. Palmer, G. (1973) Current Insights into the Active Center of Spinach Ferredoxin and Other Iron-sulfur proteins, in *Iron-Sulfur Proteins* (Lovenberg, W., Ed.), pp 285−325, Academic Press, New York.
44. Ragan, C. I., Galante, Y. M., Hatefi, Y., and Ohnishi, T. (1982) Resolution of mitochondrial NADH dehydrogenase and isolation of two iron-sulfur proteins. *Biochemistry 21*, 590–594.
45. Bungert, S., Krafft, B., Schlesinger, R., and Friedrich, T. (1999) One-step purification of the NADH dehydrogenase fragment of the *Escherichia coli* complex I by means of Strep-tag affinity chromatography. *FEBS Lett. 460*, 207–211.
46. Berks, B. C., Ferguson, S. J., Moir, J. W., and Richardson, D. J. (1995) Enzymes and associated electron transport systems that catalyse the respiratory reduction of nitrogen oxides and oxyanions. *Biochim. Biophys. Acta 1232*, 97–173.
47. Pohl, T., Bauer, T., Dörner, K., Stolpe, S., Sell, P., Zocher, G., and Friedrich, T. (2007) Iron-sulfur cluster N7 of the NADH: ubiquinone oxidoreductase (complex I) is essential for stability but not involved in electron transfer. *Biochemistry 46*, 6588–6596.
48. Nakamaru-Ogiso, E., Yano, T., Yagi, T., and Ohnishi, T. (2005) Characterization of the iron-sulfur cluster N7 (N1c) in the subunit NuoG of the proton-translocating NADH-quinone oxidoreductase from *Escherichia coli*. *J. Biol. Chem. 280*, 301–307.
49. Page, C. C., Moser, C. C., Chen, X., and Dutton, P. L. (1999) Natural engineering principles of electron tunnelling in biological oxidation-reduction. *Nature 402*, 47–52.
50. Peters, J. W., Lanzilotta, W. N., Lemon, B. J., and Seefeldt, L. C. (1998) X-ray crystal structure of the Fe-only hydrogenase (CpI) from *Clostridium pasteurianum* to 1.8 angstrom resolution. *Science 282*, 1853–1858.
51. Dyall, S. D., Yan, W., Delgadillo-Correa, M. G., Lunceford, A., Loo, J. A., Clarke, C. F., and Johnson, P. J. (2004) Non-mitochondrial complex I proteins in a hydrogenosomal oxidoreductase complex. *Nature 431*, 1103–1107.
52. Hrdy, I., Hirt, R. P., Dolezal, P., Bardonová, L., Foster, P. G., Tachezy, J., and Embley, T. M. (2004) Trichomonas hydrogenosomes contain the NADH dehydrogenase module of mitochondrial complex I. *Nature 432*, 618–622.

53. Boxma, B., de Graaf, R. M., van der Staay, G. W. M., van Alen, T. A., Ricard, G., Gabaldón, T., van Hoek, A. H. A. M., Moon-van der Staay, S. Y., Koopman, W. J. H., van Hellemond, J. J., Tielens, A. G. M., Friedrich, T., Veenhuis, M., Huynen, M. A., and Hackstein, J. H. P. (2005) An anaerobic mitochondrion that produces hydrogen. *Nature 434*, 74–79.
54. Boxma, B., Ricard, G., van Hoek, A. H. A. M., Severing, E., Moon-van der Staay, S.-Y., van der Staay, G. W. M., van Alen, T. A., de Graaf, R. M., Cremers, G., Kwantes, M., McEwan, N. R., Newbold, C. J., Jouany, J.-P., Michalowski, T., Pristas, P., Huynen, M. A., and Hackstein, J. H. P. (2007) The [FeFe] hydrogenase of *Nyctotherus ovalis* has a chimeric origin. *BMC Evol. Biol. 7*, 230.
55. Yano, T., Sled, V. D., Ohnishi, T., and Yagi, T. (1996) Expression and characterization of the flavoprotein subcomplex composed of 50-kDa (NQO1) and 25-kDa (NQO2) subunits of the proton-translocating NADH-quinone oxidoreductase of *Paracoccus denitrificans*. *J. Biol. Chem. 271*, 5907–5913.
56. Velazquez, I., Nakamaru-Ogiso, E., Yano, T., Ohnishi, T., and Yagi, T. (2005) Amino acid residues associated with cluster N3 in the NuoF subunit of the proton-translocating NADH-quinone oxidoreductase from *Escherichia coli*. *FEBS Lett. 579*, 3164–3168.
57. Fecke, W., Sled, V. D., Ohnishi, T., and Weiss, H. (1994) Disruption of the gene encoding the NADH-binding subunit of NADH: ubiquinone oxidoreductase in *Neurospora crassa*. Formation of a partially assembled enzyme without FMN and the iron-sulphur cluster N-3. *Eur. J. Biochem. 220*, 551–558.
58. Sled, V. D., Friedrich, T., Leif, H., Weiss, H., Meinhardt, S. W., Fukumori, Y., Calhoun, M. W., Gennis, R. B., and Ohnishi, T. (1993) Bacterial NADH-quinone oxidoreductases: Iron-sulfur clusters and related problems. *J. Bioenerg. Biomembr. 25*, 347–356.
59. Chatelet, C., Gaillard, J., Pétillot, Y., Louwagie, M., and Meyer, J. (1999) A [2Fe-2S] protein from the hyperthermophilic bacterium *Aquifex aeolicus*. *Biochem. Biophys. Res. Commun. 261*, 885–889.
60. Yeh, A. P., Chatelet, C., Soltis, S. M., Kuhn, P., Meyer, J., and Rees, D. C. (2000) Structure of a thioredoxin-like [2Fe-2S] ferredoxin from *Aquifex aeolicus*. *J. Mol. Biol. 300*, 587–595.

BI801307N